Waveguide QED: Many-body bound-state effects in coherent and Fock-state scattering from a two-level system

Huaixiu Zheng,[1,2] Daniel J. Gauthier,[1] and Harold U. Baranger[1,2,*]
[1]*Department of Physics, Duke University, P.O. Box 90305, Durham, North Carolina 27708, USA*
[2]*Center for Theoretical and Mathematical Sciences, Duke University, Durham, North Carolina 27708, USA*
(Received 1 October 2010; published 14 December 2010)

Strong coupling between a two-level system (TLS) and bosonic modes produces dramatic quantum optics effects. We consider a one-dimensional continuum of bosons coupled to a single localized TLS, a system which may be realized in a variety of plasmonic, photonic, or electronic contexts. We present the exact many-body scattering eigenstate obtained by imposing open boundary conditions. *Multiphoton bound states* appear in the scattering of two or more photons due to the coupling between the photons and the TLS. Such bound states are shown to have a large effect on scattering of both Fock- and coherent-state wave packets, especially in the intermediate coupling-strength regime. We compare the statistics of the transmitted light with a coherent state having the same mean photon number: as the interaction strength increases, the one-photon probability is suppressed rapidly, and the two- and three-photon probabilities are greatly enhanced due to the many-body bound states. This results in non-Poissonian light.

DOI: 10.1103/PhysRevA.82.063816 PACS number(s): 42.50.Ct, 03.65.Nk, 78.67.Uh, 42.50.Gy

I. INTRODUCTION

Recently, there has been increasing interest in designing quantum optical elements based on the strong coupling between light and matter [1–9]. The strong-coupling regime has been realized in the classic cavity quantum electrodynamics (QED) systems [10–12], as well as in circuit QED experiments [13–16]. Several experimental systems have been proposed for realizing devices such as a single-photon transistor [4,8] and a quantum switch [6,7,17], including surface plasmons coupled to a single two-level emitter [4], a superconducting transmission line resonator coupled to a local superconducting charge qubit [6,7], and propagating photons in a one-dimensional (1D) waveguide coupled to a TLS [18,19]. Most of the theoretical work focuses on a single-photon coupled to a local quantum system modeled as a TLS. The key property used in the device proposals is that, if the energy of the incident photon is tuned to be on resonance with the TLS, the system will block the transmission of photons due to destructive interference between the directly transmitted photon and the photon re-emitted by the impurity [4,6].

A more challenging task is to study the two-photon (or more) scattering problem in such systems. The two-photon problem has been addressed by Shen and Fan using a generalized Bethe ansatz [18,19]. They showed that two-photon bound states emerge as the photons interact with the TLS. Effective attractive and repulsive interactions can be induced depending on the energy of the photons [18]. Such effective interactions between photons may provide new avenues for controlling photon entanglement [20]. However, the scattering eigenstates were not constructed explicitly in Ref. [19]: the bound states were found by first constructing Bethe-type scattering eigenstates and then deducing the bound states via the completeness of the basis. It is difficult to generalize the method in Ref. [19] to solve the three-photon (or more) scattering problem, in which we expect more complicated and interesting photon correlations.

Here, we present a method to explicitly construct exact n-photon scattering eigenstates and then use the eigenstates to analyze the scattering of Fock- and coherent-state wave packets. The system consists of a 1D bosonic continuum coupled to a local TLS as shown in Fig. 1. First, we explicitly construct the n-photon ($n = 1$ to 4) scattering eigenstates by imposing open boundary conditions while requiring that the incoming wave functions consist entirely of plane waves [21,22]. In addition to two-photon bound states, three-photon bound states appear in the three-photon scattering eigenstates, and likewise, n-photon bound states appear in the n-photon scattering eigenstates. Second, to show the significance of these bound states in the scattering of practical light sources, we study the scattering of one-, two-, and three-photon Fock-state wave packets. It is shown that the two- and three-photon bound states dramatically enhance the transmission of two- and three-photon wave packets, respectively. Third, we study the scattering of coherent states to determine the impact of the bound states on both the photon correlation and the statistics of the transmitted and reflected photons. Strong bunching and antibunching effects appear, and the statistics are non-Poissonian.

The paper is organized as follows. In Sec. II, we introduce the model, solve for the n-photon scattering eigenstates in the $n = 1$ to $n = 4$ cases, and construct the corresponding S matrix based on the Lippmann-Schwinger formalism [23]. In Sec. III, the impact of bound states on photon transmission is studied

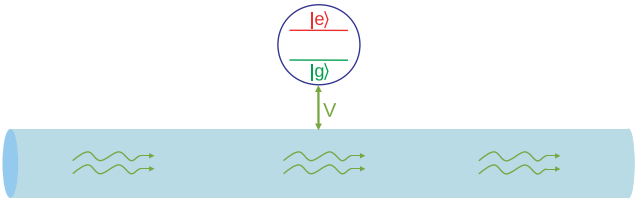

FIG. 1. (Color online) Sketch of the structure considered: a 1D continuum of bosons coupled to a two-level system.

*harold.baranger@duke.edu

for initial Fock-state wave packets with photon numbers of one, two, and three. In Sec. IV, we present the analysis of photon correlation and statistics for coherent-state scattering. Finally, we conclude in Sec. V.

II. SCATTERING EIGENSTATES

The system we study consists of a TLS coupled to photons propagating in both directions in a 1D waveguide [9,18,19]. The system is modeled by the Hamiltonian [18]

$$H = \int dx \frac{1}{i}\left[a_R^\dagger(x)\frac{d}{dx}a_R(x) - a_L^\dagger(x)\frac{d}{dx}a_L(x)\right] + \left(\epsilon - \frac{i\Gamma'}{2}\right)|e\rangle\langle e| + \int dx V\delta(x) \times \{[a_R^\dagger(x) + a_L^\dagger(x)]S^- + \text{H.c.}\}, \quad (1)$$

where $a_R^\dagger(x)/a_L^\dagger(x)$ is the creation operator for a right-going (left-going) photon at position x, ϵ is the level splitting between the ground state $|g\rangle$ and the excited state $|e\rangle$ of the TLS, Γ' is the decay rate into channels other than the 1D continuum, V is the frequency-independent coupling strength, and $S^- = |g\rangle\langle e|$ is the atomic lowering operator. Throughout the paper, we set the group velocity c and Plank's constant $\hbar$ to 1 for simplicity.

It is natural to transform to modes which are either even or odd about the origin, $a_e^\dagger(x) \equiv [a_R^\dagger(x) + a_L^\dagger(-x)]/\sqrt{2}$ or $a_o^\dagger(x) \equiv [a_R^\dagger(x) - a_L^\dagger(-x)]/\sqrt{2}$. The Hamiltonian (1) is then decomposed into two decoupled modes: $H = H_e + H_o$, with

$$H_e = \int dx \frac{1}{i}a_e^\dagger(x)\frac{d}{dx}a_e(x) + (\epsilon - i\Gamma'/2)|e\rangle\langle e| + \int dx \bar{V}\delta(x)\,[a_e^\dagger(x)S^- + \text{H.c.}], \quad (2a)$$

$$H_o = \int dx \frac{1}{i}a_o^\dagger(x)\frac{d}{dx}a_o(x), \quad (2b)$$

where the effective coupling strength becomes $\bar{V} = \sqrt{2}V$. Note that the odd mode is free. The number operator for even bosons is $n_e = \int dx a_e^\dagger(x)a_e(x)$, that for odd bosons is $n_o = \int dx a_o^\dagger(x)a_o(x)$, and the occupation number of the TLS is $n_{tls} = |e\rangle\langle e|$. Because H commutes with certain number operators, $[H, n_e + n_{tls}] = [H, n_o] = 0$, the total numbers of excitations in both the even and the odd spaces are separately conserved. We now focus on finding the nontrivial even-mode solution and then transform back to the left (right) representation.

An n-excitation state in the even space ($n = n_e + n_{tls}$) is given by

$$|\psi_n\rangle = \int dx_1 \cdots dx_n g_n(x_1,\ldots,x_n)a_e^\dagger(x_1)\cdots a_e^\dagger(x_n)|0,g\rangle + \int dx_1 \cdots dx_{n-1} e_n(x_1,\ldots,x_{n-1}) \times a_e^\dagger(x_1)\cdots a_e^\dagger(x_{n-1})|0,e\rangle, \quad (3)$$

where $|0,g\rangle$ is the 0-photon state with the atom in the ground state. From $H_e|\psi_n\rangle = E_n|\psi_n\rangle$, we obtain the Schrödinger equations

$$\left[\frac{1}{i}(\partial_1 + \cdots + \partial_n) - E_n\right]g_n(x_1,\ldots,x_n) + \frac{\bar{V}}{n}[\delta(x_1)e_n(x_2,\ldots,x_n) + \cdots + \delta(x_n)e_n(x_1,\ldots,x_{n-1})] = 0,$$
$$\left[\frac{1}{i}(\partial_1 + \cdots + \partial_{n-1}) - E_n + \epsilon - i\Gamma'/2\right]e_n(x_1,\ldots,x_{n-1}) + n\bar{V}g_n(0,x_1,\ldots,x_{n-1}) = 0, \quad (4)$$

where the eigenvalue $E_n = k_1 + k_2 + \cdots k_n$, and $g_n(x_1,\ldots,x_n)$ is discontinuous at $x_i = 0, i = 1,\ldots,n$. In all the following calculations, we set $g_n(0,x_1,\ldots,x_{n-1}) = [g_n(0^+,x_1,\ldots,x_{n-1}) + g_n(0^-,x_1,\ldots,x_{n-1})]/2$ [21,22]. The scattering eigenstates $g_n(x_1,\ldots,x_n)$ and $e_n(x_1,\ldots,x_{n-1})$ are constructed by imposing the boundary condition that, in the incident region, $g_n(x_1,\ldots,x_n)$ is the free-bosonic plane wave. That is, for $x_1,\ldots,x_n < 0$,

$$g_n(x_1,\ldots,x_n) = \frac{1}{n!}\sum_Q h_{k_1}(x_{Q_1})\cdots h_{k_n}(x_{Q_n}), \quad (5a)$$

$$h_k(x) = \frac{1}{\sqrt{2\pi}}e^{ikx}. \quad (5b)$$

For $n = 1$, plane-wave solutions are sufficient to satisfy Eq. (4) with eigenenergy $E = k$:

$$g_1(x) = g_k(x) = h_k(x)[\theta(-x) + \bar{t}_k\theta(x)], \quad (6a)$$

$$e_1 = \frac{i}{2\sqrt{\pi}V}(\bar{t}_k - 1), \quad (6b)$$

$$\bar{t}_k = \frac{k - \epsilon + i\Gamma'/2 - i\Gamma_c/2}{k - \epsilon + i\Gamma'/2 + i\Gamma_c/2}, \quad (6c)$$

where $\theta(x)$ is the step function and $\Gamma_c = \bar{V}^2 = 2V^2$ is the spontaneous emission rate from the TLS to the 1D continuum. Note that $\bar{t}_k$ is the transmission coefficient for the even problem; because the even mode is chiral, $|\bar{t}_k| = 1$ when $\Gamma' = 0$.

For $n = 2$, plane-wave solutions are not sufficient to satisfy Eq. (4). As discussed by Shen and Fan [18,19], a two-photon bound state must be included to guarantee the completeness of the basis. Here, instead of extracting the bound state through a completeness check [18,19], we construct the scattering eigenstate explicitly and find a two-photon bound-state contribution to the solution, as has been done in the open interacting resonant-level model [21]. We require the two-photon solution to satisfy Eq. (5a) in the region $x_1, x_2 < 0$ and solve for the solution in other regions using Eq. (4). This method of constructing scattering eigenstates can be generalized to cases of three, four, and even more photons. In the Appendix, it is shown that the two-photon eigenstate with eigenenergy $E = k_1 + k_2$ is

$$g_2(x_1,x_2) = g_{k_1,k_2}(x_1,x_2) = \frac{1}{2!}\left[\sum_Q g_{k_1}(x_{Q_1})g_{k_2}(x_{Q_2}) + \sum_{PQ} B^{(2)}_{k_{P_1},k_{P_2}}(x_{Q_1},x_{Q_2})\theta(x_{Q_1})\right], \quad (7a)$$

$$e_2(x) = \frac{\sqrt{2}i}{V}[g_2(0^+,x) - g_2(0^-,x)], \quad (7b)$$

$$B^{(2)}_{k_{P_1},k_{P_2}}(x_{Q_1},x_{Q_2}) \equiv -(\bar{t}_{k_{P_1}}-1)(\bar{t}_{k_{P_2}}-1)h_{k_{P_1}}(x_{Q_2})h_{k_{P_2}}(x_{Q_2}) \times e^{(-\Gamma/2-i\epsilon)|x_{Q2}-x_{Q1}|}\theta(x_{Q_2}-x_{Q_1}). \quad (7c)$$

Here, $P=(P_1,P_2)$ and $Q=(Q_1,Q_2)$ are permutations of (1,2) needed to account for the bosonic symmetry of the wave function, and $\Gamma=\Gamma_c+\Gamma'$ is the total spontaneous emission rate. The two-body bound-state term $B^{(2)}_{k_{P_1},k_{P_2}}(x_{Q1},x_{Q2})\theta(x_{Q_1})$ is generated when there are two photons interacting with the same TLS, while the TLS can only absorb one photon at one time. The binding strength of the two photons depends on the total spontaneous emission rate Γ. Conceptually, two photons have two ways of going through the TLS. One is to pass by the TLS independently as plane waves and gain a phase factor, which is described by the first term of $g_2(x_1,x_2)$. The other way is to bind together and form a bound state, which is described by the second term. The formation of the bound state can be viewed as a result of stimulated emission: the first photon excites the TLS and the passing of the second photon stimulates emission of the first photon into the same state, hence producing the bound state.

For $n=3$, a procedure similar to that used to solve the $n=2$ case yields

$$g_3(x_1,x_2,x_3)=g_{k_1,k_2,k_3}(x_1,x_2,x_3)=\frac{1}{3!}\Bigg[\sum_Q g_{k_1}(x_{Q_1})g_{k_2}(x_{Q_2})g_{k_3}(x_{Q_3})+\sum_{PQ} g_{k_{P_1}}(x_{Q_1})B^{(2)}_{k_{P_2},k_{P_3}}(x_{Q_2},x_{Q_3})\theta(x_{Q_2}) + \sum_{PQ} B^{(3)}_{k_{P_1},k_{P_2},k_{P_3}}(x_{Q_1},x_{Q_2},x_{Q_3})\theta(x_{Q_1})\Bigg], \quad (8a)$$

$$e_3(x_1,x_2)=\frac{3i}{\sqrt{2}V}[g_3(0^+,x_1,x_2)-g_3(0^-,x_1,x_2)], \quad (8b)$$

$$B^{(3)}_{k_{P_1},k_{P_2},k_{P_3}}(x_{Q_1},x_{Q_2},x_{Q_3}) \equiv 2(\bar{t}_{k_{P_1}}-1)(\bar{t}_{k_{P_2}}-1)(\bar{t}_{k_{P_3}}-1)h_{k_{P_1}}(x_{Q_2})h_{k_{P_2}}(x_{Q_3})h_{k_{P_3}}(x_{Q_3})e^{(-\Gamma/2-i\epsilon)|x_{Q_3}-x_{Q_1}|}\theta(x_{Q_{32}})\theta(x_{Q_{21}}), \quad (8c)$$

where $P=(P_1,P_2,P_3)$ and $Q=(Q_1,Q_2,Q_3)$ are permutations of (1,2,3) and $\theta(x_{Q_{ij}})=\theta(x_{Q_i}-x_{Q_j})$ for short. In addition to the two-photon bound state, there emerges a three-body bound state, $B^{(3)}_{k_{P_1},k_{P_2},k_{P_3}}(x_{Q_1},x_{Q_2},x_{Q_3})\theta(x_{Q_1})$, in the region $x_1,x_2,x_3>0$. Conceptually, there are three ways for the three photons to pass by the atom: (i) all three photons propagate as independent plane waves; (ii) two photons form a two-body bound state, while the other one propagates independently as a plane wave; and (iii) all three photons bind together and form a three-body bound state. These three processes are described by the first, second, and third terms of $g_3(x_1,x_2,x_3)$, respectively.

This simple picture can be applied to a general n-photon scattering process. For example, in the case of four-photon scattering, there are five ways for the four photons to pass by the atom as illustrated in Fig. 2: (i) all four propagate as independent plane waves; (ii) two photons form a two-body bound state, while the other two propagate independently as plane waves; (iii) three photons form a three-body bound state, while the other one propagates independently as a plane wave; (iv) four photons form two independent two-body bound states; and (v) four photons form a four-body bound state. These five processes can be identified as the five terms of $g_4(x_1,x_2,x_3,x_4)$ in the four-photon solution, which is given by

$$g_4(x_1,x_2,x_3,x_4)=\frac{1}{4!}\Bigg[\sum_Q g_{k_1}(x_{Q_1})g_{k_2}(x_{Q_2})g_{k_3}(x_{Q_3})g_{k_4}(x_{Q_4})+\sum_{PQ} g_{k_{P_1}}(x_{Q_1})g_{k_{P_2}}(x_{Q_2})B^{(2)}_{k_{P_3},k_{P_4}}(x_{Q_3},x_{Q_4})\theta(x_{Q_3}) + \sum_{PQ} g_{k_{P_1}}(x_{Q_1})B^{(3)}_{k_{P_2},k_{P_3},k_{P_4}}(x_{Q_2},x_{Q_3},x_{Q_4})\theta(x_{Q_2})+\sum_{PQ} B^{(2)}_{k_{P_1},k_{P_2}}(x_{Q1},x_{Q_2})B^{(2)}_{k_{P_3},k_{P_4}}(x_{Q_3},x_{Q_4})\theta(x_{Q_1})\theta(x_{Q_3}) + \sum_{PQ} B^{(4)}_{k_{P_1},k_{P_2},k_{P_3},k_{P_4}}(x_{Q_1},x_{Q_2},x_{Q_3},x_{Q_4})\theta(x_{Q_1})\Bigg], \quad (9a)$$

$$e_4(x_1,x_2,x_3)=\frac{4i}{\sqrt{2}V}[g_4(0^+,x_1,x_2,x_3)-g_4(0^-,x_1,x_2,x_3)], \quad (9b)$$

$$B^{(4)}_{k_{P_1},k_{P_2},k_{P_3},k_{P_4}}(x_{Q_1},x_{Q_2},x_{Q_3},x_{Q_4}) \equiv -2^2(\bar{t}_{k_{P_1}}-1)(\bar{t}_{k_{P_2}}-1)(\bar{t}_{k_{P_3}}-1)(\bar{t}_{k_{P_4}}-1)h_{k_{P_1}}(x_{Q_2})h_{k_{P_2}}(x_{Q_3})h_{k_{P_3}}(x_{Q_4})h_{k_{P_4}}(x_{Q_4}) \times e^{(-\Gamma/2-i\epsilon)|x_{Q_4}-x_{Q_1}|}\theta(x_{Q_4}-x_{Q_3})\theta(x_{Q_3}-x_{Q_2})\theta(x_{Q_2}-x_{Q_1}). \quad (9c)$$

The scattering eigenstates of a general n-photon problem can be constructed recursively in a similar way: the only unknown term in $g_n(x_1,\ldots,x_n)$ is the n-photon bound state, as all the other terms can be constructed from the solutions of the $1-,2-,\ldots,(n-1)$-photon problems. We extrapolate from the results of $n=2$–4 that, in general ($n\geqslant 2$), the n-body

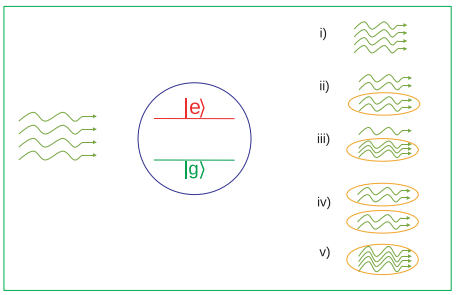

FIG. 2. (Color online) Schematic of different processes in four-photon scattering by a two-level system. Plane waves are represented by (green) wiggly lines, while many-body bound states are represented by (orange) ovals.

bound state assumes the form

$$B_{k_1,\ldots,k_n}(x_1,\ldots,x_n) = -(-2)^{n-2}\prod_{i=1}^{n}\left(\bar{t}_{k_i}-1\right)\prod_{i=1}^{n-1}\theta(x_{i+1}-x_i) \times h_{k_1}(x_n)h_{k_2}(x_2)\cdots h_{k_{n-1}}(x_{n-1})h_{k_n}(x_n) \times e^{(-\Gamma/2-i\epsilon)|x_n-x_1|}. \quad (10)$$

We have verified this expression for $n=5$. Thus we have given explicit formulas for constructing the exact n-photon scattering eigenstates.

The exact scattering eigenstates can be used to construct the scattering matrix. According to the Lippmann-Schwinger formalism [23], one can read off the "in" state (before scattering) and the "out" state (after scattering) of a general n-photon S matrix from $g_n(x_1,\ldots,x_n)$ in the input region $(x_1<0,\ldots,x_n<0)$ and in the output region $(x_1>0,\ldots,x_n>0)$, respectively. The in and out states of one- and two-photon scattering matrices are given by

$$\left|\phi_{\text{in}}^{(1)}\right\rangle_e = \int dx h_k(x)a_e^\dagger(x)|0\rangle, \quad (11a)$$

$$\left|\phi_{\text{out}}^{(1)}\right\rangle_e = \int dx \bar{t}_k h_k(x)a_e^\dagger(x)|0\rangle, \quad (11b)$$

and

$$\left|\phi_{\text{in}}^{(2)}\right\rangle_e = \int dx_1dx_2\frac{1}{2!}\left[\sum_Q h_{k_1}(x_{Q_1})h_{k_2}(x_{Q_2})\right]a_e^\dagger(x_1)a_e^\dagger(x_2)|0\rangle,$$

$$\left|\phi_{\text{out}}^{(2)}\right\rangle_e = \int dx_1dx_2\frac{1}{2!}\left[\sum_Q \bar{t}_{k_1}\bar{t}_{k_2}h_{k_1}(x_{Q_1})h_{k_2}(x_{Q_2}) + \sum_{PQ} B_{k_{P_1},k_{P_2}}(x_{Q_1},x_{Q_2})\right]a_e^\dagger(x_1)a_e^\dagger(x_2)|0\rangle, \quad (12)$$

and similarly for three and four photons. The corresponding S matrices are

$$S_e^{(n)} = \int dk_1\cdots dk_n\frac{1}{n!}\left|\phi_{\text{out}}^{(n)}\right\rangle_{ee}\left\langle\phi_{\text{in}}^{(n)}\right|. \quad (13)$$

Note that the unitarity of the S matrix is automatically satisfied since the incoming state $|\phi_{\text{in}}^{(n)}\rangle_e$ is a complete basis set in the even space [19,23].

The S matrix in the odd space is just the identity operator because the odd mode is free and decoupled from the impurity and the even mode,

$$S_o^{(n)} = \int dk_1\cdots dk_n\frac{1}{n!}\left|\phi_{\text{in}}^{(n)}\right\rangle_{o\,o}\left\langle\phi_{\text{in}}^{(n)}\right|, \quad (14a)$$

$$\left|\phi_{\text{in}}^{(n)}\right\rangle_o = \int dx_1\cdots dx_n\frac{1}{n!}\sum_Q\prod_{i=1}^{n}h_{k_i}(x_{Q_i})a_e^\dagger(x_i)|0\rangle. \quad (14b)$$

Finally, we wish to construct the scattering matrix in the right-left representation based on the S matrices in the even-odd representation. For a general n-photon scattering problem, the possible scattering channels are that i photons undergo scattering in the even space and $n-i$ photons undergo scattering in the odd space, with i running from 0 to n. In addition, the even and odd spaces are decoupled from each other. Therefore, the n-photon S matrix is

$$S^{(n)} = \sum_{i=0}^{n}S_e^{(i)}\otimes S_o^{(n-i)}. \quad (15)$$

We use this S matrix to study the scattering of Fock states and coherent-state wave packets in the right and left spaces in subsequent sections.

III. SCATTERING OF FOCK STATES

To show the significance of the many-body bound states, we study the scattering of a Fock state off of a TLS. We assume that the incident mode propagates to the right and the TLS is initially in the ground state. We use the S matrices defined in Eq. (15) to evaluate the transmission and reflection coefficients. In practice, any state that contains a finite number of photons must have the form of a wave packet. Thus, we start with the definition of the continuous-mode photon wave-packet creation operator in momentum space [24],

$$a_\alpha^\dagger = \int dk\alpha(k)a^\dagger(k)|0\rangle, \quad (16)$$

with the normalization condition $\int dk|\alpha(k)|^2=1$. The corresponding continuous-mode n-photon Fock state is

$$|n_\alpha\rangle = \frac{(a_\alpha^\dagger)^n}{\sqrt{n!}}|0\rangle, \quad (17)$$

and the output state after it scatters off the TLS is

$$\left|\text{out}_\alpha^{(n)}\right\rangle = S^{(n)}|n_\alpha\rangle. \quad (18)$$

To obtain the scattering probabilities of a Fock state from the S matrix found in Sec. II, we use the following general procedure. (i) First, we write an n-photon input Fock state traveling to the right in momentum space: $|n_\alpha\rangle = (1/\sqrt{n!})\int dk_1\cdots dk_n\,\alpha(k_1)\cdots\alpha(k_n)|k_1,\ldots,k_n\rangle$. (ii) Next, we apply the S matrix to the input state and find the output state $|\text{out}_\alpha^{(n)}\rangle = S^{(n)}|n_\alpha\rangle = (1/\sqrt{n!})\int dk_1\cdots dk_n\,\alpha(k_1)\cdots\alpha(k_n)S^{(n)}|k_1,\ldots,k_n\rangle$ in the even-odd basis. (iii) We transform back to the right-left basis. Then we project the output state onto the n-photon (right- and left-going) momentum basis $|k_1,\ldots,k_n\rangle_R,\ldots,|k_1,\ldots,k_i\rangle_R\otimes|k_{i+1},\ldots,k_n\rangle_L,\ldots,|k_1,\ldots,k_n\rangle_L$ and take the absolute value square to obtain the probabilities $P(k_1,\ldots,k_n)$ of finding

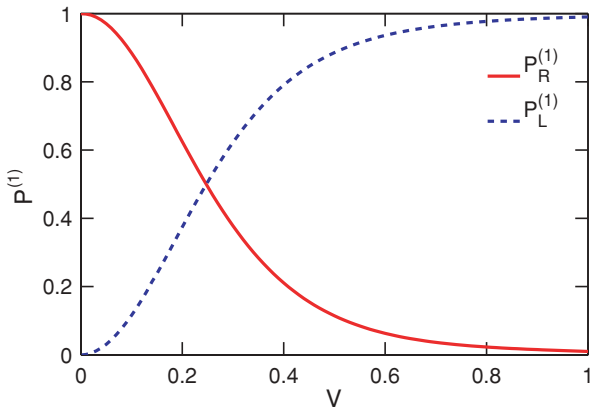

FIG. 3. (Color online) Single-photon transmission ($P_R^{(1)}$) and reflection ($P_L^{(1)}$) probabilities as a function of coupling strength V. The incident photon is on resonance with the two-level system ($k_0 = \epsilon$) and we have considered the lossless case $\Gamma' = 0$. $\Delta = 0.1$.

the output state in $|k_1, \ldots, k_n\rangle$. (iv) Finally, we integrate $P(k_1, \ldots, k_n)$ over $k_1, \ldots, k_n$ to obtain the total transmission and reflection probabilities. Here, a right-going (left-going) state is defined by a positive (negative) momentum; that is, $k_1 > 0, \ldots, k_n > 0$ for $|k_1, \ldots, k_n\rangle_R$ and $k_1 < 0, \ldots, k_n < 0$ for $|k_1, \ldots, k_n\rangle_L$.

For convenience, we choose Gaussian-type wave packets with the spectral amplitude

$$\alpha(k) = (2\pi\Delta^2)^{-1/4} \exp\left(-\frac{(k-k_0)^2}{4\Delta^2}\right). \tag{19}$$

For all of the numerical examples in this paper, we choose $k_0 = \epsilon$: the central frequency of the wave packet is on resonance with the TLS, a condition which makes the interaction between the photons and the TLS strongest. We take the central momentum $k_0 \gg \Delta$ so that the narrow-band condition is satisfied. In particular, we choose $\Delta = 0.1$. However, we emphasize that all the conclusions we draw are independent of the choice of Δ. That is because all the transmission and reflection probabilities are functions of Γ_c/Δ and Γ'/Δ, where $\Gamma_c = 2V^2$. A different choice of Δ does not change any of the qualitative results, but merely rescales the spontaneous emission rates.

A. Single-photon Fock-state scattering

The probabilities of transmission ($P_R^{(1)}$) and reflection ($P_L^{(1)}$) for a single-photon Fock state are found as

$$P_R^{(1)} = \int_{k>0} dk\ \left|\langle k|\mathrm{out}_\alpha^{(1)}\rangle\right|^2 = \int_{k>0} dk\ \alpha(k)^2 |t_k|^2, \tag{20a}$$

$$P_L^{(1)} = \int_{k<0} dk\ \left|\langle k|\mathrm{out}_\alpha^{(1)}\rangle\right|^2 = \int_{k>0} dk\ \alpha(k)^2 |r_k|^2, \tag{20b}$$

where $t_k = (\bar{t}_k + 1)/2$, $r_k = (\bar{t}_k - 1)/2$, and $\bar{t}_k$ is the transmission coefficient already defined for the even mode [Eq. (6a)].

Note that the propagation of a single photon is strongly modulated by the TLS as we turn on the coupling, as shown in Fig. 3. In the strong-coupling limit, a single photon is perfectly reflected and the two-level atom acts as a mirror. This perfect reflection is due to destructive interference between the directly transmitted state and the state re-emitted from the TLS. A single-photon transistor [4] and a quantum switch [6] have been proposed based on this perfect reflection.

B. Two-photon Fock-state scattering

For two incident photons, following the general procedure already outlined, we find that the transmission and reflection probabilities are

$$P_{RR}^{(2)} = \int_{k_1>0,k_2>0} dk_1 dk_2\ \frac{1}{2!}\left|\langle k_1,k_2|\mathrm{out}_\alpha^{(2)}\rangle\right|^2, \tag{21a}$$

$$P_{RL}^{(2)} = \int_{k_1>0,k_2<0} dk_1 dk_2\ \left|\langle k_1,k_2|\mathrm{out}_\alpha^{(2)}\rangle\right|^2, \tag{21b}$$

$$P_{LL}^{(2)} = \int_{k_1<0,k_2<0} dk_1 dk_2\ \frac{1}{2!}\left|\langle k_1,k_2|\mathrm{out}_\alpha^{(2)}\rangle\right|^2, \tag{21c}$$

where $P_{RR}^{(2)}$, $P_{RL}^{(2)}$, and $P_{LL}^{(2)}$ are, respectively, the probability for two photons to be transmitted (right-going), one to be transmitted and one reflected, and two photons to be reflected (left-going).

To show the significance of the bound state in the propagation of multiphoton Fock states, we separate each of the probabilities $P_{RR}^{(2)}$, $P_{RL}^{(2)}$, and $P_{LL}^{(2)}$ into two parts. One part is the contribution from only the plane-wave term (labeled PW), which is the direct transmission or reflection. The other is the contribution from all the other terms (labeled BS), including the bound-state term as well as the interference term between the plane wave and the bound state. Note that the BS part vanishes in the absence of the bound state, as in the case of single-photon scattering. Therefore, it is a manifestation of the nonlinear effect caused by the interaction between the TLS and two or more photons. As an example, $P_{RR}^{(2)}$ split into the plane-wave and bound-state parts is

$$P_{RR}^{(2)} = \int_{k_1>0,k_2>0} dk_1 dk_2 |t(k_1,k_2) + B(k_1,k_2)|^2 \tag{22a}$$

$$= \left(P_{RR}^{(2)}\right)_{\mathrm{PW}} + \left(P_{RR}^{(2)}\right)_{\mathrm{BS}}, \tag{22b}$$

$$\left(P_{RR}^{(2)}\right)_{\mathrm{PW}} = \int_{k_1>0,k_2>0} dk_1 dk_2 |t(k_1,k_2)|^2, \tag{22c}$$

$$\left(P_{RR}^{(2)}\right)_{\mathrm{BS}} = \int_{k_1>0,k_2>0} dk_1 dk_2 [t^*(k_1,k_2)B(k_1,k_2) + t(k_1,k_2)B^*(k_1,k_2) + |B(k_1,k_2)|^2], \tag{22d}$$

$$t(k_1,k_2) = \alpha(k_1)\alpha(k_2)t_{k_1}t_{k_2}, \tag{22e}$$

$$B(k_1,k_2) = \left[\frac{-i/2\pi}{k_1 - \epsilon + \frac{i\Gamma}{2}} + \frac{-i/2\pi}{k_2 - \epsilon + \frac{i\Gamma}{2}}\right] \times \int_{k'>0} dk' \alpha(k')\alpha(k_1 + k_2 - k') r_{k'} r_{k_1+k_2-k'}. \tag{22f}$$

Figure 4 shows the three transmission probabilities $P_{RR}^{(2)}$, $P_{RL}^{(2)}$, and $P_{LL}^{(2)}$ for our standard parameters, with the contributions from the plane wave and bound state plotted separately in Figs. 4(a)–4(c). *Note that the presence of the bound state has a very substantial effect on these transmission probabilities.* As shown in Figs. 4(a) and 4(b), $P_{RR}^{(2)}$ and $P_{RL}^{(2)}$ are enhanced by the formation of the bound state. This is mainly due to constructive

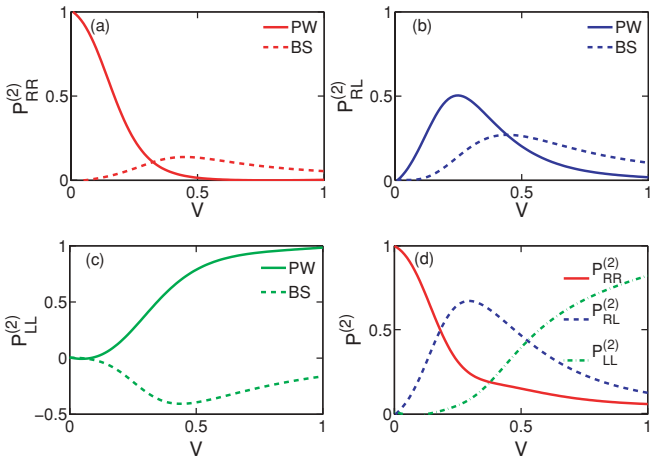

FIG. 4. (Color online) Two-photon transmission and reflection probabilities as a function of coupling strength V. (a) Probability that both photons are transmitted (and hence are right-going; $P^{(2)}_{RR}$). (b) Probability that one photon is transmitted and one reflected (right-left; $P^{(2)}_{RL}$). (c) Probability that both photons are reflected (both left-going; $P^{(2)}_{LL}$). (d) The three processes in a single plot. The label PW refers to the contribution from the plane-wave term only, while BS refers to all the other contributions involving bound-state terms. Incident photons are on resonance with the TLS ($k_0 = \epsilon$), we consider the lossless case $\Gamma' = 0$, and $\Delta = 0.1$. Note the large effect of the bound state on these quantities.

interference between the plane wave and the bound state. In contrast, Fig. 4(c) shows that $P^{(2)}_{LL}$ is strongly reduced in the presence of the bound state because of destructive interference between the plane wave and the bound state (change from ~0.8 to ~0.4 at $V = 0.5$). Therefore, the presence of the bound state tends to *increase* one-photon and two-photon transmission, while *decreasing* two-photon reflection.

A particularly interesting aspect of the results in Fig. 4 is that the effect of the bound state is most prominent in the *intermediate*-coupling regime, not at the strongest coupling. This is because, first, in the weak-coupling limit, the interaction is too weak to produce a pronounced bound state for two-photon scattering, and, second, in the strong-coupling limit, the TLS responds to the first photon too quickly (over a duration of order $1/\Gamma$ with $\Gamma = 2V^2$) for the second photon to produce a significant nonlinear effect. (The formation of the bound state requires the presence of both photons in the TLS.) The optimal coupling strength V_m for producing nonlinear (bound-state) effects lies at intermediate coupling, when the spontaneous emission rate Γ is of the order of the wave-packet width Δ ($V_m \sim 0.4$ when $\Delta = 0.1$).

C. Three-photon Fock-state scattering

Following the general procedure for obtaining scattering probabilities, the transmission and reflection probabilities for three-photon Fock-state scattering are defined as

$$
\begin{aligned}
P^{(3)}_{RRR} &= \int_{k_1>0,k_2>0,k_3>0} dk_1 dk_2 dk_3 \, \frac{1}{3!} \left|\langle k_1,k_2,k_3 | \mathrm{out}^{(3)}_\alpha \rangle\right|^2, \\
P^{(3)}_{RRL} &= \int_{k_1>0,k_2>0,k_3<0} dk_1 dk_2 dk_3 \, \frac{1}{2!} \left|\langle k_1,k_2,k_3 | \mathrm{out}^{(3)}_\alpha \rangle\right|^2, \\
P^{(3)}_{RLL} &= \int_{k_1>0,k_2<0,k_3<0} dk_1 dk_2 dk_3 \, \frac{1}{2!} \left|\langle k_1,k_2,k_3 | \mathrm{out}^{(3)}_\alpha \rangle\right|^2, \\
P^{(3)}_{LLL} &= \int_{k_1<0,k_2<0,k_3<0} dk_1 dk_2 dk_3 \, \frac{1}{3!} \left|\langle k_1,k_2,k_3 | \mathrm{out}^{(3)}_\alpha \rangle\right|^2,
\end{aligned}
\tag{23}
$$

where $P^{(3)}_{RRR}$, $P^{(3)}_{RRL}$, $P^{(3)}_{RLL}$, and $P^{(3)}_{LLL}$ are the probabilities of three photons being transmitted (all right-going), two being transmitted and one reflected, one being transmitted and two reflected, and all three being reflected (left-going), respectively. As in the two-photon scattering case, we separate each probability into two parts: the contribution from only the plane-wave term and the contribution from all the other terms, including the bound states as well as the interference between the plane wave and the bound states. The probabilities and the decomposition into plane-wave and bound-state parts are plotted in Fig. 5 for our usual parameters.

Figure 5 shows that the bound-state contribution to the transmission probabilities is, as for two photons, very substantial. In Figs. 5(a) and 5(b), the bound-state parts of $P^{(3)}_{RRR}$ and $P^{(3)}_{RRL}$ are positive; thus, these probabilities are enhanced by the bound states. Figure 5(d) shows that $P^{(3)}_{LLL}$ is suppressed by the bound-state contribution for an arbitrary coupling strength. In contrast, as we increase the coupling strength, $P^{(3)}_{RLL}$ is first suppressed and then enhanced by the bound-state part as shown in Fig. 5(c). Tuning the coupling strength changes the relative phase between the plane-wave and the bound-state parts; for $P^{(3)}_{RLL}$, the interference between them happens to change from destructive to constructive as the coupling strength increases.

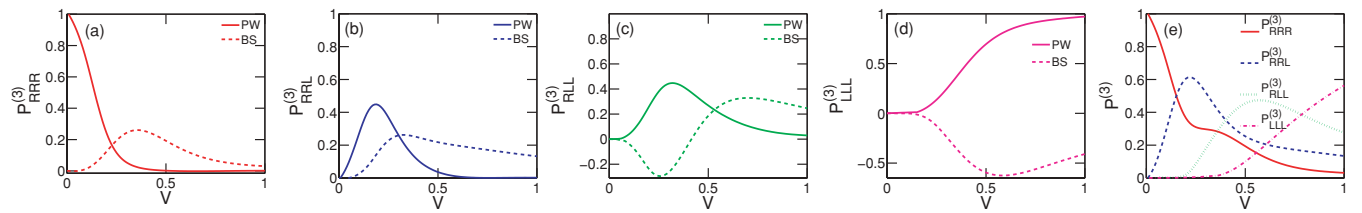

FIG. 5. (Color online) Three-photon transmission and reflection probabilities as a function of coupling strength V. (a) Probability of all three photons being transmitted ($P^{(3)}_{RRR}$). (b) Probability of two photons being transmitted and one reflected ($P^{(3)}_{RRL}$). (c) Probability of one photon being transmitted and two photons reflected ($P^{(3)}_{RLL}$). (d) Probability of all three photons being reflected ($P^{(3)}_{LLL}$). (e) P^3 values shown all together. The label PW refers to the contribution from only the plane-wave term, while BS refers to all the other contributions, involving bound-state terms. Incident photons are on resonance with the TLS ($k_0 = \epsilon$), we consider the lossless case $\Gamma' = 0$, and $\Delta = 0.1$. Note the large bound-state effects.

Finally, as in the two-photon case, the most pronounced bound-state effects occur in the intermediate-coupling regime instead of the strong-coupling limit.

To sum up this section, we point out that all the curves plotted in Figs. 3–5 are universal in terms of the choice of Δ. Because Δ appears in the scattering probabilities ($P_R^{(1)}$, etc.) only in the ratio Γ_c/Δ and Γ'/Δ, a different choice of Δ (i.e., other than the 0.1 used in Figs. 3–5) is equivalent to rescaling V and does not change the shape of the curves. Therefore, the substantial bound-state effects observed here are intrinsic for multiphoton scattering processes in this system, independent of the details of the wave packets.

IV. SCATTERING OF COHERENT-STATES

We now turn to studying the scattering of coherent states, to show, first, the strong photon-photon correlation induced by the the TLS and, second, the change in photon number statistics. The incident coherent-state wave packet is defined by [24]

$$|\alpha\rangle = e^{a_\alpha^\dagger - \bar{n}/2}|0\rangle, \tag{24}$$

with $a_\alpha^\dagger = \int dk\alpha(k)a^\dagger(k)|0\rangle$, and mean photon number $\bar{n} = \int dk|\alpha(k)|^2$. A Gaussian-type wave packet is chosen,

$$\alpha(k) = \frac{\sqrt{\bar{n}}}{(2\pi\Delta^2)^{1/4}} \exp\left[-\frac{(k-k_0)^2}{4\Delta^2}\right]; \tag{25}$$

for numerical evaluations, we use, as before, $\Delta = 0.1$ and $k_0 = \epsilon \gg \Delta$. The output state $|\text{out}_\alpha\rangle$ is then

$$|\text{out}_\alpha\rangle = \sum_n S^{(n)}|\alpha\rangle. \tag{26}$$

We assume that the incident coherent state is right-going and the TLS is in the ground state initially. We present the analysis of second-order correlation and photon number statistics in the transmitted field.

A. Correlation

The second-order correlation function of the transmitted field is defined as [24]

$$g_R^{(2)}(x_2-x_1) = \frac{\langle \text{out}_\alpha|a_R^\dagger(x_1)a_R^\dagger(x_2)a_R(x_2)a_R(x_1)|\text{out}_\alpha\rangle}{\langle \text{out}_\alpha|a_R^\dagger(x_1)a_R(x_1)|\text{out}_\alpha\rangle^2}. \tag{27}$$

We consider the mean photon number $\bar{n} \leqslant 1.0$. In this case, the probability of finding $n \geqslant 3$ number states is much lower than that of finding $n = 2$ number states. Moreover, the contributions from $n \geqslant 3$ states to $g^{(2)}$ are at least 1 order of Δ (=0.1) smaller than that from the $n = 2$ state. Therefore, we neglect the contributions from $n \geqslant 3$ number states. The second-order correlation function simplifies to

$$g_R^{(2)}(x_2 - x_1) = \frac{\left|\int dk_1 dk_2 \alpha(k_1)\alpha(k_2)\left(t_{k_1}t_{k_2} - r_{k_1}r_{k_2}e^{-\frac{\Gamma(x_2-x_1)}{2}}\right)\right|^2}{\left|\int dk_1 dk_2 \alpha(k_1)\alpha(k_2)t_{k_1}t_{k_2}\right|^2}. \tag{28}$$

The contributions from the directly transmitted state and the bound state can be identified as the first term and second term in the numerator of $g_R^{(2)}(x_2 - x_1)$ in Eq. (28). In the absence of the bound state, $g_R^{(2)}(x_2 - x_1)$ is always equal to unity. As we turn on the interaction, the interference between the directly transmitted state and the bound state will give rise to interesting correlation behavior. Figure 6 shows the second-order correlation as a function of $\Gamma(x_2 - x_1)$ at various coupling strengths, V, with the 1D mode with $\Gamma' = 0.1$. In the weak-coupling limit ($V = 0.16$), as shown in Fig. 6(a), the directly transmitted state dominates and $g_R^{(2)}(0)$ is slightly smaller than 1. We observe a slight initial antibunching. As V increases [Figs. 6(b) and 6(c)], $g_R^{(2)}(0)$ decreases further and the initial antibunching gets stronger; it is strongest at $V = 0.34$ when $g_R^{(2)}(0) = 0$. Note that the antibunching is getting weaker as one moves away from the origin for $V \leqslant 0.34$. Further increase in V starts to change the initial antibunching [$V = 0.38$, $g_R^{(2)}(0) < 1$] to bunching [$V = 0.45$, $g_R^{(2)}(0) > 1$] as shown in Figs. 6(d)–6(f). In this case, the bound state starts to dominate the correlation behavior. It is remarkable that, for $V > 0.34$, the initial antibunching ($V < 0.40$) or bunching ($V > 0.40$) is followed by a later antibunching $g_R^{(2)}(0) = 0$, which is caused by the cancellation of the directly transmitted state and the bound state. The formation of the bound state gives rise to a rich phenomenon of photon-photon correlation, which is very sensitive to the coupling strength V to the 1D mode. *Effective attractive or repulsive interaction between photons is induced by the presence of a single TLS* [18].

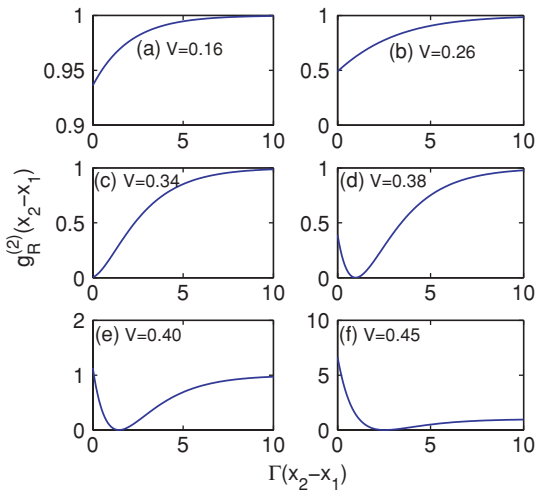

FIG. 6. (Color online) Second-order correlation of the transmitted field, given an incident coherent state with $\bar{n} \leqslant 1$ at various coupling strengths V, with the 1D continuum. (a) $V = 0.16$, (b) $V = 0.26$, (c) $V = 0.34$, (d) $V = 0.38$, (e) $V = 0.40$, and (f) $V = 0.45$. The spontaneous emission rate to channels other than the 1D continuum is set to $\Gamma' = 0.10$. Note that the correlation behavior is very sensitive to the coupling strength to the 1D continuum, showing both bunching and antibunching.

Our findings agree with the results obtained by Chang *et al.* [4] using a very different approach. In the lossless $\Gamma' = 0$ case, as we increase the coupling strength, the transmission of individual photons is reduced rapidly [see, e.g., Figs. 3 and 4(a)]. But the two-photon bound state can strongly enhance the transmission. Therefore, we will observe a strong initial bunching followed by a later antibunching, similar to Fig. 6(f).

B. Photon number distribution

Given the output state $|\text{out}_\alpha\rangle$, we measure the photon number distribution in the transmitted field following the general procedure described in Sec. III.

$$\begin{aligned} P_0 &= |\langle \text{out}_\alpha|(|0\rangle_R \otimes |I\rangle_L)|^2, \\ P_1 &= \int_{k>0} dk |\langle \text{out}_\alpha|(|k\rangle_R \otimes |I\rangle_L)|^2, \\ P_2 &= \int_{k_1,k_2>0} dk_1 dk_2 \frac{1}{2!} |\langle \text{out}_\alpha|(|k_1,k_2\rangle_R \otimes |I\rangle_L)|^2, \\ P_3 &= \int_{k_1,k_2,k_3>0} dk_1 dk_2 dk_3 \frac{1}{3!} |\langle \text{out}_\alpha|(|k_1,k_2,k_3\rangle_R \otimes |I\rangle_L)|^2, \end{aligned} \tag{29}$$

where $|I\rangle_L$ is the complete basis set in the left-going photon space. We consider a mean photon number $\bar{n} \leqslant 1.0$ in the incident coherent state. In this case, the probability of finding the four-photon state is negligible ($\leqslant 1.6\%$). We compare the photon number distribution P_n of the output state with the $(P_n)_{\text{Poisson}}$ of a coherent state having the same mean photon number.

Figure 7 shows the ratio between $(P_n)_{\text{Poisson}}$ and P_n as a function of the coupling strength V and the mean photon number $\bar{n}$ of the incident coherent state. The 0-photon probability does not deviate much from that of a coherent state in the entire parameter region we considered. The one-photon probability is lower than the corresponding probability in a coherent state. In contrast, the two- and three-photon probabilities are much higher than those in a coherent state, especially in the strong-coupling regime. That is, the interaction between photons and the TLS redistributes the probabilities among different photon numbers. *The one-photon probability is reduced and is redistributed to the two- and three-photon probabilities.* This is mainly because the bound states enhance the transmission of multiphoton states, as we have shown in Secs. III B and III C. In conclusion, we obtain a non-Poissonian light source after the scattering. It is perhaps possible to use this strongly correlated light source to perform a passive decoy-state quantum key distribution to raise the key generation rate [25–28].

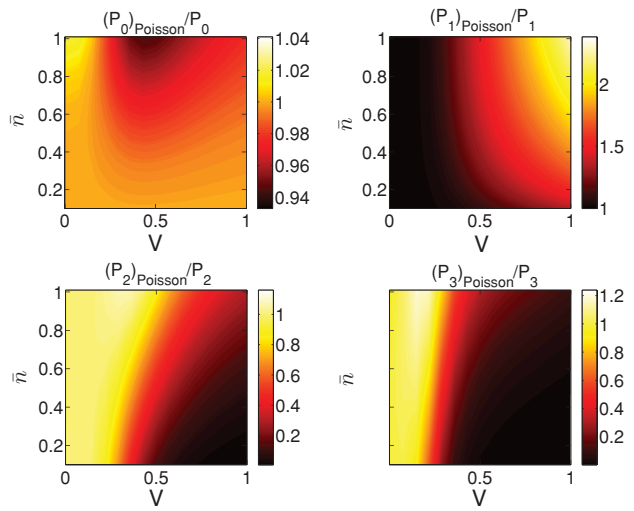

FIG. 7. (Color online) Photon number distribution of the transmitted field compared with a coherent state. We considered the lossless case $\Gamma' = 0$. The statistics is non-Possonian, with the two- and three-photon content enhanced.

V. CONCLUSION

In this paper, we have presented a general method for constructing the exact scattering eigenstates for the problem of n photons interacting with a TLS. Many-body bound states appear in the presence of the coupling between photons and the TLS. Furthermore, the scattering matrices are extracted using the Lippmann-Schwinger formalism. We emphasize that the completeness of the S matrices is guaranteed by imposing open boundary conditions and requiring the incident field to be free plane waves. Based on the S matrices, we study the scattering of the Fock states and coherent states. Bound states are shown to enhance the transmission of multiphoton states and suppress the transmission of single-photon states. In the transmitted field of coherent-state scattering, photons exhibit strong bunching or antibunching effects depending on the coupling strength. This is a manifestation of the many-body bound states. Finally, we determine the photon number distribution and find that the one-photon state is transferred to two- and three-photon states. This results in a non-Poissonian light source which might have applications in quantum information.

ACKNOWLEDGMENTS

We thank H. Carmichael for valuable discussions. The work of H.U.B. was supported in part by the U.S. Office of Naval Research. H.Z. acknowledges support from the Graduate Program in Nanoscience and the Center for Theoretical and Mathematical Sciences, both of Duke University.

APPENDIX: TWO-PHOTON SCATTERING EIGENSTATE

In this appendix, we show in detail how we obtain the two-photon scattering eigenstate [Eq. (7)] by imposing the open boundary condition, Eq. (5). The equations of motion for the two-photon case read

$$\left[\frac{1}{i}(\partial_1 + \partial_2) - E_2\right] g_2(x_1,x_2) + \frac{\bar{V}}{2}[\delta(x_1)e_2(x_2) + \delta(x_2)e_2(x_1)] = 0, \tag{A1a}$$

$$\left(\frac{1}{i}\frac{d}{dx} - E_2 + \epsilon - i\Gamma'/2\right) e_2(x) + 2\bar{V} g_2(0,x) = 0, \tag{A1b}$$

which can be cast into the following set of equations:

$$\left[\frac{1}{i}(\partial_1 + \partial_2) - E_2\right] g_2(x_1,x_2) = 0, \tag{A2a}$$

$$e_2(x) = \frac{2i}{\bar{V}}[g_2(0^+,x) - g_2(0^-,x)], \tag{A2b}$$

$$\left(\frac{1}{i}\frac{d}{dx} - E_2 + \epsilon - i\Gamma'/2\right) e_2(x) + \bar{V}[g_2(0^+,x) + g_2(0^-,x)] = 0, \tag{A2c}$$

$$e_2(0^+) = e_2(0^-). \tag{A2d}$$

Here, $g_2(x_1,x_2)$ is discontinuous at $x_1 = 0, x_2 = 0$ and we set $g_2(x,0) = [g_2(x,0^+) + g_2(x,0^-)]/2$. We eliminate $e_2(x)$ from the preceding equations and obtain

$$\left[\frac{1}{i}(\partial_1 + \partial_2) - E_2\right] g_2(x_1,x_2) = 0, \tag{A3a}$$

$$\left(\frac{1}{i}\frac{d}{dx} - E_2 + \epsilon - i\Gamma'/2 - i\Gamma_c/2\right) g_2(0^+,x) = \left(\frac{1}{i}\frac{d}{dx} - E_2 + \epsilon - i\Gamma'/2 + i\Gamma_c/2\right) g_2(0^-,x), \tag{A3b}$$

$$g_2(0^+,0^+) - g_2(0^-,0^+) = g_2(0^-,0^+) - g_2(0^-,0^-). \tag{A3c}$$

Because of the bosonic symmetry, we can solve for $g_2(x_1,x_2)$ by first considering the half-space $x_1 \leqslant x_2$ and then extending the result to the full space. In this case, there are three quadrants in real space: ①$x_1 \leqslant x_2 < 0$, ②$x_1 < 0 < x_2$, and ③$0 < x_1 \leqslant x_2$. Equation (A3b) can be rewritten as two separate equations:

$$\left(\frac{1}{i}\frac{d}{dx} - E_2 + \epsilon - i\Gamma'/2 - i\Gamma_c/2\right) g_2^{②}(x,0^+) = \left(\frac{1}{i}\frac{d}{dx} - E_2 + \epsilon - i\Gamma'/2 + i\Gamma_c/2\right) g_2^{①}(x,0^-) \quad \text{for } x < 0, \tag{A4a}$$

$$\left(\frac{1}{i}\frac{d}{dx} - E_2 + \epsilon - i\Gamma'/2 - i\Gamma_c/2\right) g_2^{③}(0^+,x) = \left(\frac{1}{i}\frac{d}{dx} - E_2 + \epsilon - i\Gamma'/2 + i\Gamma_c/2\right) g_2^{②}(0^-,x) \quad \text{for } x > 0. \tag{A4b}$$

Substituting $g_2^{①}(x_1,0^-)$ [Eq. (5)] into Eq. (A4a), we solve to find

$$g_2^{②}(x,0^+) = \frac{1}{2!}\left[\bar{t}_{k_2}\frac{e^{ik_1x}}{2\pi} + \bar{t}_{k_1}\frac{e^{ik_2x}}{2\pi}\right] + Ae^{[-\Gamma/2+i(k_1+k_2-\epsilon)]x}, \tag{A5}$$

where A is a constant to be determined. Applying the constraint Eq. (A3a) to $g_2^{②}(x,0^+)$, we obtain

$$g_2^{②}(x_1,x_2) = \frac{1}{2!}\left[\bar{t}_{k_2}\frac{e^{i(k_1x_1+k_2x_2)}}{2\pi} + \bar{t}_{k_1}\frac{e^{i(k_2x_1+k_1x_2)}}{2\pi}\right] + Ae^{(\Gamma/2+i\epsilon)(x_2-x_1)}e^{i(k_1+k_2)x_1}. \tag{A6}$$

From Eq. (A6), we can identify A to be 0: otherwise, the solution is not normalizable [$e^{\Gamma(x_2-x_1)/2}$ is divergent when $x_2 - x_1 \to \infty$]. Hence, $g_2(x_1,x_2)$ in region ②is given by

$$g_2^{②}(x_1,x_2) = \frac{1}{2!}\left[\bar{t}_{k_2}\frac{e^{i(k_1x_1+k_2x_2)}}{2\pi} + \bar{t}_{k_1}\frac{e^{i(k_2x_1+k_1x_2)}}{2\pi}\right]. \tag{A7}$$

Substituting Eq. (A7) into Eq. (A4b) yields

$$g_2^{③}(0^+,x) = \frac{1}{2!}\bar{t}_{k_1}\bar{t}_{k_2}\left[\frac{e^{ik_2x}}{2\pi} + \frac{e^{ik_1x}}{2\pi}\right] + Be^{[-\Gamma/2+i(k_1+k_2-\epsilon)]x}, \tag{A8}$$

where B is a constant to be determined. Again, applying the constraint Eq. (A3a) to $g_2^{③}(0^+,x)$, we obtain

$$g_2^{③}(x_1,x_2) = \frac{1}{2!}\bar{t}_{k_1}\bar{t}_{k_2}\left[\frac{e^{i(k_1x_1+k_2x_2)}}{2\pi} + \frac{e^{i(k_1x_2+k_2x_1)}}{2\pi}\right] + Be^{(-\Gamma/2-i\epsilon)(x_2-x_1)}e^{i(k_1+k_2)x_2}. \tag{A9}$$

Finally, B is found by substituting Eqs. (5), (A7), and (A9) into the continuity condition, Eq. (A3c), yielding

$$B = -\frac{(\bar{t}_{k_1} - 1)(\bar{t}_{k_2} - 1)}{2\pi}. \tag{A10}$$

Extending these solutions from the half-space to the full space using the bosonic symmetry gives rise to the two-photon scattering eigenstate given in Eq. (7) in the text.

[1] A. Politi, M. J. Cryan, J. G. Rarity, S. Yu, and J. L. O'Brien, Science **320**, 646 (2008).

[2] M. Hofheinz, E. M. Weig, M. Ansmann, R. C. Bialczak, E. Lucero, M. Neeley, A. D. O'Connell, H. Wang, J. M. Martinis, and A. N. Cleland, Nature (London) **454**, 310 (2008).

[3] D. E. Chang, A. S. Sørensen, P. R. Hemmer, and M. D. Lukin, Phys. Rev. Lett. **97**, 053002 (2006).

[4] D. E. Chang, A. S. Sørensen, E. A. Demler, and M. D. Lukin, Nature Phys. **3**, 807 (2007).

[5] J.-Q. Liao, J.-F. Huang, Y.-X. Liu, L.-M. Kuang, and C. P. Sun, Phys. Rev. A **80**, 014301 (2009).

[6] L. Zhou, Z. R. Gong, Y.-X. Liu, C. P. Sun, and F. Nori, Phys. Rev. Lett. **101**, 100501 (2008).

[7] L. Zhou, S. Yang, Y.-X. Liu, C. P. Sun, and F. Nori, Phys. Rev. A **80**, 062109 (2009).

[8] D. Witthaut and A. S. Sørensen, New J. Phys. **12**, 043052 (2010).

[9] P. Longo, P. Schmitteckert, and K. Busch, Phys. Rev. Lett. **104**, 023602 (2010).

[10] W. Vogel, D. G. Welsch, and S. Wallentowitz, *Quantum Optics—An Introduction*, 2nd ed. (Wiley-VCH, Berlin, 2001).

[11] R. J. Thompson, G. Rempe, and H. J. Kimble, Phys. Rev. Lett. **68**, 1132 (1992).

[12] J. P. Reithmaier, G. Sek, A. Löffler, C. Hofmann, S. Kuhn, S. Reitzenstein, L. V. Keldysh, V. D. Kulakovskii, T. L. Reinecke, and A. Forchel, Nature (London) **432**, 197 (2004).

[13] A. Wallraff, D. I. Schuster, A. Blais, L. Frunzio, R.-S. Huang, J. Majer, S. Kumar, S. M. Girvin, and R. J. Schoelkopf, Nature (London) **431**, 162 (2004).

[14] I. Chiorescu, P. Bertet, K. Semba, Y. Nakamura, C. J. P. M. Harmans, and J. E. Mooij, Nature (London) **431**, 159 (2004).

[15] O. Astafiev, A. M. Zagoskin, A. A. J. Abdumalikov, Y. A. Pashkin, T. Yamamoto, K. Inomata, Y. Nakamura, and J. S. Tsai, Science **327**, 840 (2010).

[16] R. J. Schoelkopf and S. M. Girvin, Nature (London) **451**, 664 (2008).

[17] P. Longo, P. Schmittechert, and K. Busch, J. Opt. A: Pure Appl. Opt. **11**, 114009 (2009).

[18] J.-T. Shen and S. Fan, Phys. Rev. Lett. **98**, 153003 (2007).

[19] J.-T. Shen and S. Fan, Phys. Rev. A **76**, 062709 (2007).

[20] P. Maunz, D. L. Moehring, S. Olmschenk, K. C. Younge, D. N. Matsukevich, and C. Monroe, Nature Phys. **3**, 538 (2007).

[21] A. Nishino, T. Imamura, and N. Hatano, Phys. Rev. Lett. **102**, 146803 (2009).

[22] T. Imamura, A. Nishino, and N. Hatano, Phys. Rev. B **80**, 245323 (2009).
[23] J. J. Sakurai, *Modern Quantum Mechanics* (revised edition) (Addison-Wesley, Reading, MA, 1994).
[24] R. Loudon, *The Quantum Theory of Light*, 3rd ed. (Oxford University Press, New York, 2000).
[25] W.-Y. Hwang, Phys. Rev. Lett. **91**, 057901 (2003).
[26] H.-K. Lo, X. Ma, and K. Chen, Phys. Rev. Lett. **94**, 230504 (2005).
[27] X.-B. Wang, Phys. Rev. Lett. **94**, 230503 (2005).
[28] M. Curty, T. Moroder, X. Ma, and N. Lütkenhaus, Opt. Lett. **34**, 3238 (2009).